Resources and Environment 2022, 12(1): 1-10
DOI: 10.5923/j.re.20221201.01

Estimation of the Hydrological Potential of the Ungauged Watershed of Efaho (Madagascar) from the Daily Rainfall of an Average Year

Justin Ratsaramody

Laboratoire d'Hydraulique, Ecole Supérieure Polytechnique, Université d'Antsiranana, Madagascar

Abstract The waters of the Efaho River (Anosy Region, Madagascar) are planned to be diverted to provide water to the populations of this Androy Region who have been suffering from chronic drought for several decades. It was therefore necessary to know the value of the guaranteed flow in order to size the water transport pipes, but there are no recent measurements of flows to guarantee the hydraulic development. Thus, this study concerned the estimation of the hydrological potential of the ungauged Efaho catchment area, i.e. determining the average daily discharges of a year considered as an average year. On the daily rainfall data available from 01/01/1998 to 31/12/2019, two average daily rainfall years were considered as inputs for the hydrological model, namely the real average year 2000 and a fictitious average year, say 2053. The actual dry year 2016 was also considered. From the processing of these rainfall data, the physical processes (infiltration, evapotranspiration, runoff and then routing) had been reconstructed considering the characteristics of the catchment area. The implementation was carried out with the R language for data processing and with the HEC-HMS software for hydrological modelling. After comparison with some historical data, the results showed a fairly good agreement and the flow that could be used for hydraulic engineering was the flow corresponding to the first quartile of the fictitious average year 2053, i.e. 1.60 m3/s (guaranteed 274 days in the year).

Keywords Ungauged catchment, Efaho, R, HEC-HMS, SCS-CN, Fictitious average year

1. Introduction

The Efaho River (Anosy Region) is of paramount importance to the current government of Madagascar which has decided to divert its waters for the benefit of the populations living in the South of Madagascar, which has been suffering from chronic drought for decades, causing famine, extreme impoverishment, high infant mortality and even migration to other parts of Madagascar. These diverted waters will provide drinking water for the population as well as water for agricultural activities, livestock watering etc. Nevertheless, for the purposes of hydraulic design, it was essential to know the availability of the water resource provided by the catchment area at the point of capture. Indeed, if this resource was overestimated, the pipeline flows might not work; on the other hand, if this resource was underestimated, this would lead to water deprivation for the beneficiary populations.

Figure 1 shows a general location of the Efaho catchment area. The water diverted from the Efaho River is intended to be transported to Amboasary Atsimo (Figure 1).

Some historical data exist [1] but these data concern the period 1962-1974, i.e. almost 5 decades ago; moreover, these data concern only the upper part of the Efaho river catchment area but not the whole of the catchment area studied, which can then be classified in the category of ungauged catchment areas.

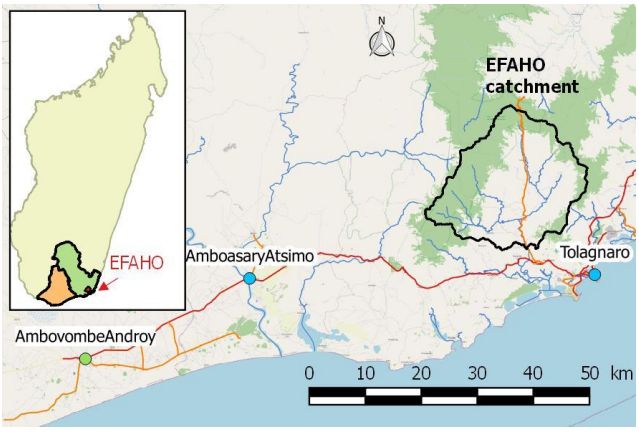

Figure 1. General location of the Efaho catchment on an Open Street Map background. The inset shows the location of the two regions (Anosy in green and Androy in orange) concerned on the island of Madagascar

In this case, the most commonly used method is a

* Corresponding author:
justinratsaramody@yahoo.fr (Justin Ratsaramody)
Received: Feb. 10, 2022; Accepted: Feb. 25, 2022; Published: Mar. 15, 2022
Published online at http://journal.sapub.org/re

regionalized method using characteristics of well-gauged basins ([2]; [3]; [4]; [5]; [6]) to deduce the characteristics of the ungauged catchment of interest. This method has given excellent results in various countries but, unfortunately, it is not applicable in our case, also due to the absence of such regionalized data.

The only way to arrive at the flow record was therefore to evaluate all the physical processes taking place in the catchment area in order to transform rainfall into flow, in other words, to use a physically based conceptualised model. This conceptualisation entails unavoidable assumptions which necessarily impact on the results. Thus, it was necessary to set "average" values for the unknown parameters and, in general, to consider an average rainfall year as input data for the watershed.

To assess the water resources of the catchment area, i.e. in order to establish the chronicle of average daily flows, the main steps of this study were

- Characterisation of the catchment area in terms of hypsometry, hydrography, pedology and land use
- Extraction of an "average" rainfall year from the processing of 21 years of daily rainfall data (01/01/1998 to 31/12/2019) but also of the dry year during this period
- Modelling of the different physical processes that lead to the reconstitution of the flows at the outlet of the Efaho catchment

2. Materials

2.1. Data for Catchment Characterisation

To characterise the catchment area, the following data were used:

- Hypsometry and Hydrography: SRTM Digital Terrain Model with a spatial resolution of 29 m at catchment latitudes (https://earthexplorer.usgs.gov)
- Land use and land cover: Compilation of ESA Sentinel-2 2020 satellite images with 10m spatial resolution [7]
- Soilology: raster file produced by the WRB (World Reference Base for Soil Resources) which is the international standard currently used by the IUSS (International Union of Soil Sciences) [8]

2.2. Weather Data

The weather data was obtained in time series format from https://giovanni.gsfc.nasa.gov :

- Daily rainfall data TRMM_3B42_Daily v7 (Tropical Rainfall Measuring Mission) covering the period 01/01/1998 to 31/12/2019
- Daily temperature data GLDAS-NOAH (Global Land Data Assimilation System) covering the period 01/01/2000 to 31/12/2019

These data are averaged over an area covering a radius of 25 km, applied to the centroid of the Efaho catchment and therefore cover the entire catchment ([9]; [10]; [11]).

2.3. Computer Tools

To carry out the calculations of the reconstruction of the chronicle of the flows at the outlet of the Efaho catchment, the following tools were used:

- GIS processing: free software QGIS (https://www.qgis.org) and SAGA (http://www.saga-gis.org)
- Programming and data processing: open source language R (https://www.r-project.org)
- Hydrological modelling: free software HEC-HMS v. 4.6.1 (*Hydrologic Engeneering Center - Hydrologic Modeling System*) available at http://www.hec.usace.army.mil/software/hec-hms

3. Methods

3.1. Catchment Characterisation

The geometric, hypsometric and hydrographic characteristics of the catchment area were obtained by processing the DTM. Land use and land cover (LULC) were obtained from the above data using the visible spectral bands (blue, green, red), the near infrared band and two shortwave infrared bands [7].

3.2. Rainfall Data Processing: Real or Fictitious Average Year

In order to determine the average daily flow record, the rainfall data used should be that of a year with "average" weather conditions, especially with regard to rainfall. To select this year of average conditions, two methods can be used:

a) Either the real average year is considered, which corresponds to the average precipitation year over the 22 years of observations (1998 to 2019)., which corresponds to the average rainfall year over the 22 years of observations (1998 to 2019)
b) Or a fictitious average year is created which is determined in the following way:
   - for each month (January, February etc.) and for the 22 years (1998 to 2019), the monthly average daily rainfall was determined
   - the month of the year corresponding to this monthly average thus constitutes the month of the fictitious year which is then composed month by month in this way

The average year thus determined, whether real or fictitious, will then be the daily rainfall series that will constitute the input data for the hydrological modelling. By proceeding in this way, exaggerations are avoided that could have been caused by the great variability of rainfall from one year to the next. Nevertheless, the dry year is also considered, i.e. the year with the lowest annual value among

the years of observation.

3.3. Assessment of Evapotranspiration

Rainfall loss rates through evapotranspiration can be high in the dry season [1], so it was essential to take this into account.

For the calculation of potential evapotranspiration (PET), the formula of Hamon ([12], [13]) was adopted:

$$PET = \frac{29.8 N e_s(T)}{T + 273.2}$$
$$\text{where } e_s(T) = 0.6108 \exp\left[\frac{17.27T}{T + 273.3}\right] \quad (1)$$

PET : potential evapotranspiration (mm); e_s : saturation vapour pressure (Pa); T : mean temperature (°C); N : number of hours of sunshine given by

$$N = 2 \arccos\left[-\tan\phi \tan\delta\right] \frac{12}{\pi}$$
$$\text{where } \delta = 1 + 0.033 \cos\left(\frac{2\pi}{365} J\right) \quad (2)$$

φ: latitude; δ: declination and J: Julian day

The PET assumes that the amount of water available for this evapotranspiration is unlimited. The actual evapotranspiration (AEP) is then calculated as follows:

$$\begin{cases} AEP = PET & \text{if } P > PET \\ AEP = 0 & \text{if } P < PET \end{cases} \quad (3)$$

P (mm): average daily rainfall. The calculation time step is therefore the day for the different equations (1) to (3).

3.4. Modelling of Rainfall-Runoff Transformation Processes

3.4.1. SCS-CN Runoff Model

In this work, the SCS-CN (*Soil Conservation Service - Curve Number*) runoff model was adopted which, although empirical in nature, is one of the most widely used methods in the world due to its high agreement between theoretical results and observed values. Another reason for its popularity is that the model depends on a single parameter, CN, which reflects the hydrological impacts of land use, land cover and infiltration capacity. The SCS-CN model is based on the water balance equation [14]:

$$P = I_a + F + R \quad (4)$$

P: rainfall (mm); I_a : initial abstraction (mm); F: cumulative infiltration (mm) which does not include I_a and R is direct runoff (mm).

With the additional assumption of a direct relationship between the initial abstraction and the maximum abstraction potential, S, it leads ([14]; [15])

$$\frac{R}{P - I_a} = \frac{F}{S} \text{ and } I_a = \lambda S \quad (5)$$

S: maximum retention potential (mm) after the beginning of runoff and λ is a regional parameter depending on geographical and climatic factors [14]. In its original form [16], the regional parameter is λ =0.2 which leads to the fundamental equation of the SCS-CN model:

$$\begin{cases} R = \dfrac{(P - 0.2S)^2}{P + 0.8S} & \text{if } P > 0.2S \\ R = 0 & \text{if } P < 0.2S \end{cases} \quad (6)$$

To calculate S, the empirical relationship between S and CN is ([15], [17]):

$$S = \frac{25400}{CN} - 254 \quad (7)$$

As the excess rainfall does not instantaneously turn into runoff, the latter only occurs after a lag time which, for ungauged catchments, is estimated by the SCS as [18]:

$$T_{lag} = 0.6 T_c \quad (8)$$

where T_c is the time of concentration.

The time of concentration T_c was evaluated (for each of the sub-catchments) according to Passini's relationship (valid for rural watersheds with a surface area of over 4000 ha):

$$T_c = 1.44 \frac{(AL)^{1/3}}{\sqrt{S}} \quad (9)$$

A: Catchment area [ha]; L: Length of longest flow path [m]; S: Slope [%]; T_c : Time of concentration [min].

For normal (moisture) conditions, the CN, denoted $CN(II)$, is given by equation (7). For different past conditions prior to the date of calculation, the following relationships exist [16]:

$$CN(I) = \frac{4.2 CN(II)}{10 - 0.058 CN(II)}$$
$$CN(III) = \frac{23 CN(II)}{10 - 0.12 CN(II)} \quad (10)$$

$CN(I)$: for dry antecedent conditions and $CN(III)$, for wet antecedent conditions. Generally, these conditions are for 5 days before the current day.

3.4.2. Baseflow Modelling

Researchers have already addressed the issue of determining baseflow, e.g. [19] for Ontario (Canada), unfortunately all proposed methods were based on the existence of regional data with gauged catchments. Thus, in the absence of measurements, this baseflow was evaluated monthly as being the flow corresponding to 15% of the flows calculated without base flows, an arbitrary but realistic value in view of the impermeable behaviour of the basin [1] in which the water tables play a minor role.

3.5. Hydrograph Routing Modelling

In general, the routing of hydrographs of flows at the outlet of the various sub-catchments is based on the Saint-Venant equations [20]

$$\frac{\partial A}{\partial t}+\frac{\partial \mathrm{Q}}{\partial \mathrm{x}}=q_L$$
$$\frac{1}{g}\frac{\partial V}{\partial t}+\frac{V}{g}\frac{\partial V}{\partial x}+\frac{\partial y}{\partial x}=S_0-S_f \quad (11)$$

where S_f = energy line slope; S_0 = bed slope; V = velocity; y = hydraulic depth; x = distance along the flow path; t = time; g = acceleration due to gravity; q_L : lateral flow per unit length.

In the present study, the model adopted was the Muskingum model which is obtained by combining the continuity equation and the diffusive representation of the Saint-Venant momentum equation, i.e. by neglecting the convective acceleration $(V/g)(\partial V/\partial x)$ and the local acceleration $(1/g)(\partial V/\partial t)$ in the dynamic equation i.e.:

$$S_f = S_0 - \frac{\partial y}{\partial x} \quad (12)$$

The Muskingum model ultimately takes the form of 2 equations which are the continuity equation and the storage equation at a time t [21]:

$$\frac{dS_t}{dt} = I_t - O_t \quad (13)$$

$$S_t = K\left[XI_t + (1-X)O_t\right] \quad (14)$$

I_t : inflow to the reach (m3/s); O_t : outflow from the reach (m3/s); S_t : storage in the reach (m3); K is the storage constant (sec) and X is the weighting factor (-) between the inflow and the outflow.

For routing, both equations (13) and (14) have to be numerically integrated. And at each time step and at each computational space step, the K and X parameters of the Muskingum model are recalculated based on the properties of the routing channel and the flow depth. This is necessary to ensure the stability and convergence conditions of the numerical integration (CFL condition).

4. Results

4.1. Catchment Characteristics

The characteristics of the Efaho River catchment are shown in Figures 2, 3 and 4.

Figure 3 shows the distribution of the HSG (Hydrologic Soil Group) runoff classes over the catchment: it can be seen that the catchment has a fairly high runoff potential. Indeed, the HSG are classified from A to D by order of increasing impermeability and Table 1 shows that the whole catchment is of high impermeability.

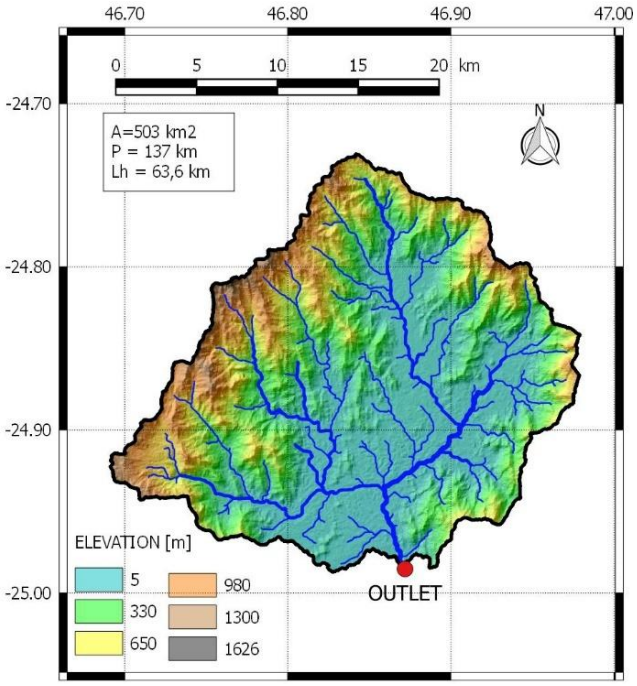

Figure 2. Hypsometry and Hydrography of the Efaho catchment. Lh=63.6 km is the hydraulic length of the main river

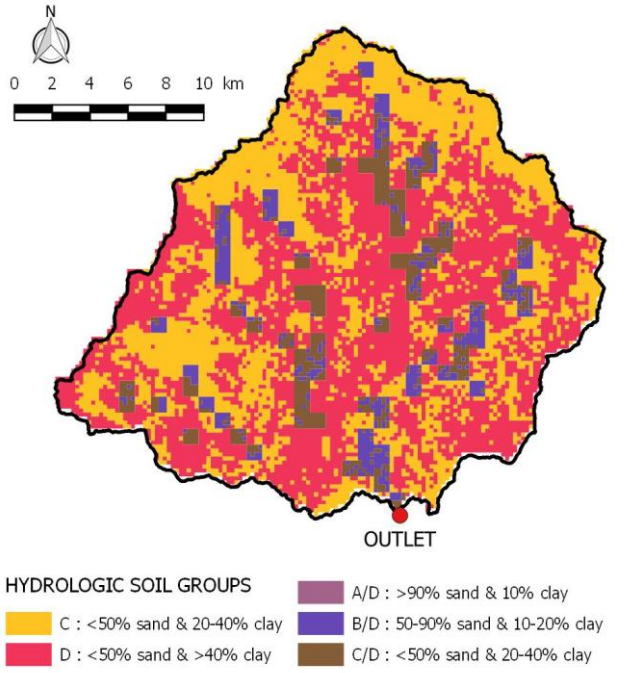

Figure 3. Hydrological soil classes (HSG) of the EFAHO catchment: very high impermeability (dominance of Class C and Class D)

Table 1. Distribution of HSG Classes in the Efaho catchment

HSG Class	A (km2)	A (%)
C	192.04	38.1
D	239.96	47.7
C/D	31.05	6.2
D/D	40.35	8.0

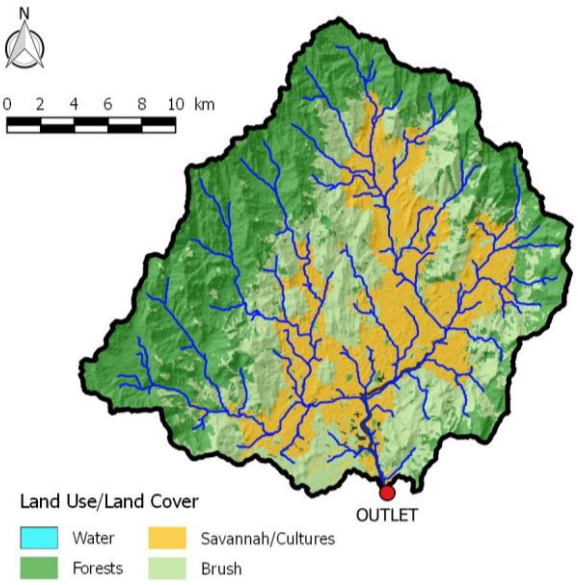

Figure 4. Land use and land cover in the Efaho catchment

4.2. Results of Meteorological Data Processing

4.2.1. Distribution of Interannual Daily Rainfall

This distribution is shown in Table 2 which shows that the average year was 2000 (2013 mm annual rainfall) while the driest year was 2016 (with an annual rainfall of 468 mm).

Table 2. Distribution of annual rainfall in the Efaho catchment from 1998 to 2019

Year	P [mm]	Year	P [mm]	Year	P [mm]
1998	1392	2006	722	2014	980
1999	1069	2007	740	2015	960
2000	**1013**	2008	588	**2016**	**468**
2001	1075	2009	1153	2017	1040
2002	1177	2010	862	2018	773
2003	777	2011	1160	2019	1343
2004	1176	2012	1021		
2005	**1540**	2013	1068		

Furthermore, using a liner regression, there is a general downward trend in the amount of annual rainfall over the 22 years of observations (Figure 5).

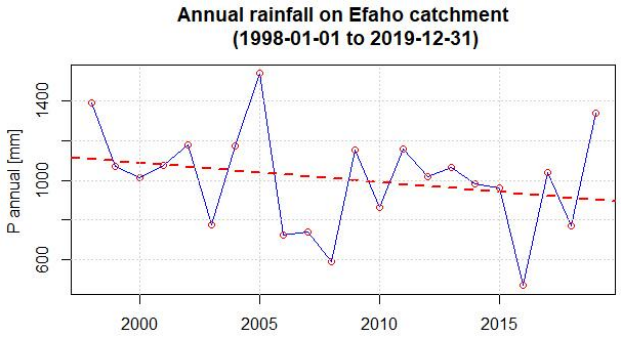

Figure 5. Temporal variation of annual rainfall in the Efaho catchment. Red dashed line: regression line indicating the overall trend

4.2.2. Actual Average Year and Fictitious Average Year

Using the procedure described in § 3.2, these are the actual average year 2000 and the fictitious average year 2053 (a non-leap year date assigned quite randomly). These two time series are shown in Figure 6 and 7, respectively.

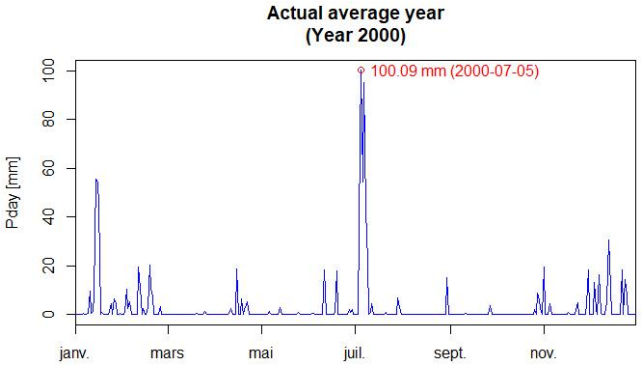

Figure 6. Actual average year (year 2000). Annual total = 1013.1 mm; maximum value: 100.09 mm occurred on 05 July 2000

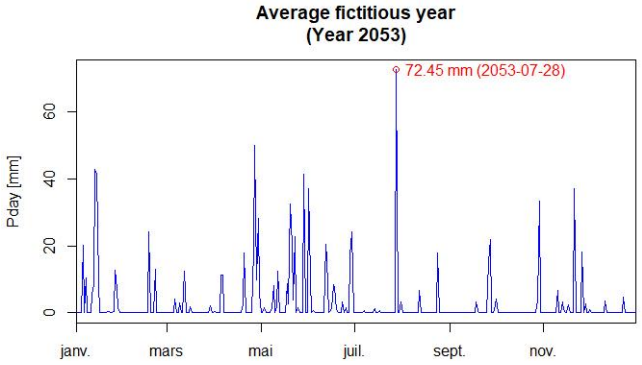

Figure 7. Fictitious average year. Annual total = 971.5 mm; maximum value: 72.5 mm on 28 July

Between the two average years, real and fictitious, there is a difference of 1013.1 - 971.5 = 41.6 mm which represents 41.6/1013.1 = 4.1%. This difference can be considered negligible. On the other hand, Figure 6 and Figure 7 are very different with regard to the temporal distribution of daily rainfall. Their only common point is that the maximum daily rainfall occurs in July (yet in the middle of the dry season in Madagascar).

4.2.3. Results of Evapotranspiration Calculations

By applying the relationships (1) to (3) with the data of the fictitious average year, the values of actual evapotranspiration (AEP) shown in Figure 8 with the daily rainfall distribution were obtained:

The maximum daily AEP (2.36 mm) occurs on the same date as the maximum daily rainfall of the average fictitious year, i.e. on 28 July 2053 (see Figure 7), as this is the date when the amount of rainfall available for evapotranspiration is maximum. The AEP for the actual mean year (2000) and the dry year (2016) have the same pattern as in Figure 8 and are not presented here. However, the following annual ratios can be noted:

- Average fictitious year 2053: AEP/P = 116.71 mm/953.42 mm = 0.12
- Actual average year 2000: AEP/P = 116.9 mm/1013.8 mm = 0.115
- Actual dry year 2016: AEP/P = 71.35 mm/467.93 mm = 0.15

These results show that, at least for the annual balances, the AEP represents 11.5 to 15% of the total rainfall, a result that can be used for a quick assessment.

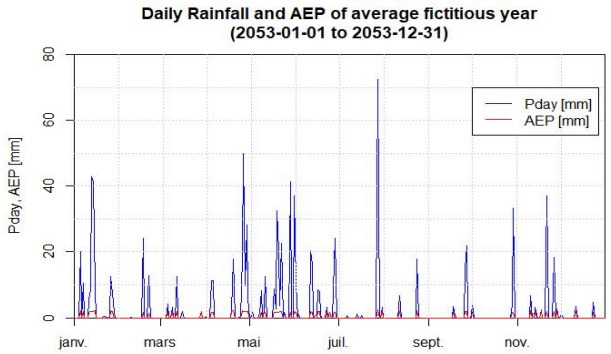

Figure 8. Distribution of daily rainfall and AEP for the fictitious average year

4.3. Hydrological Modelling Results

4.3.1. Division into Sub-Catchments

In order to carry out the hydrological modelling, the Efaho catchment was divided into 13 sub-catchments (SBV) shown in Figure 9:

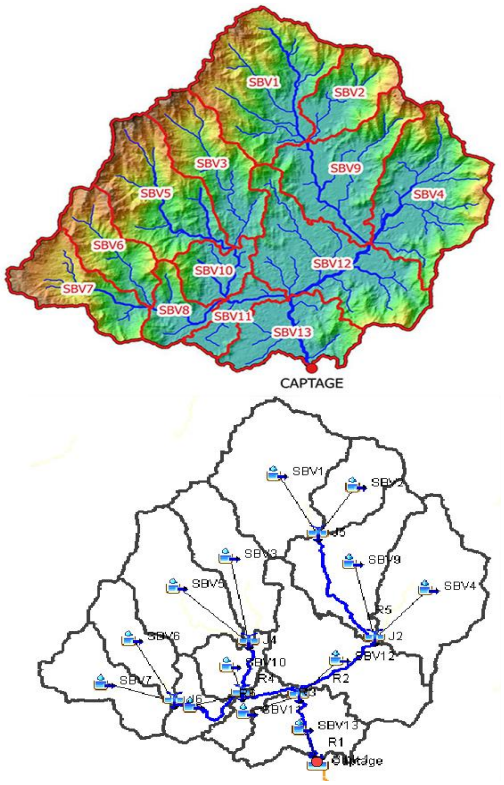

Figure 9. Sub-catchments of the hydrological modelling. Top: representation in real space. Bottom: schematic representation in HEC-HMS

Table 3 gives the characteristics of these sub-catchments as well as the lag time and time of concentration calculated from equations (8) and (9).

Table 3. Characteristics of the sub-catchments in the hydrological modelling

SBV	Aire (km2)	Lag [min]	Tc [min]	SBV	Aire (km2)	Lag [min]	Tc [min]
SBV1	65,56	75,76	126,26	SBV8	16,16	51,45	85,74
SBV2	26,20	50,74	84,57	SBV9	48,84	82,90	138,17
SBV3	39,33	63,00	105,00	SBV10	17,77	172,39	287,32
SBV4	62,82	79,47	132,44	SBV11	13,05	190,36	317,27
SBV5	51,25	60,61	101,01	SBV12	64,88	150,26	250,43
SBV6	27,28	41,01	68,36	SBV13	32,82	277,04	461,73
SBV7	32,90	42,57	70,96				

4.3.2. CN values for Sub-Catchments

The normal CN values (CN(II)) for each of the sub-catchments are given in Table 4.

Table 4. Average CN values per SBV

SBV	CN II	SBV	CN II
SBV1	76.07	SBV8	76.97
SBV2	76.69	SBV9	77.96
SBV3	75.90	SBV10	77.99
SBV4	76.78	SBV11	78.51
SBV5	75.32	SBV12	77.23
SBV6	75.33	SBV13	74.51
SBV7	75.35		

When calculating flows, the CN(I) and/or CN(III) values will be used depending on the previous moisture conditions (equation (10)).

4.3.3. Final Results

For the three years studied, Figures 10 to 12 show the variation of the average daily flows at the catchment site (outlet of the total catchment) considering the base flow (15% of the calculated flow):

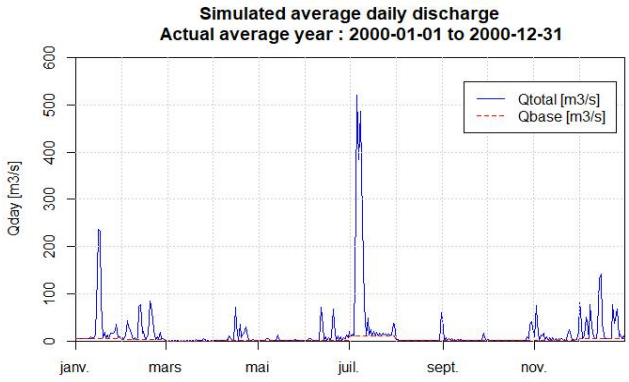

Figure 10. Average daily flows for the actual average year (year 2000)

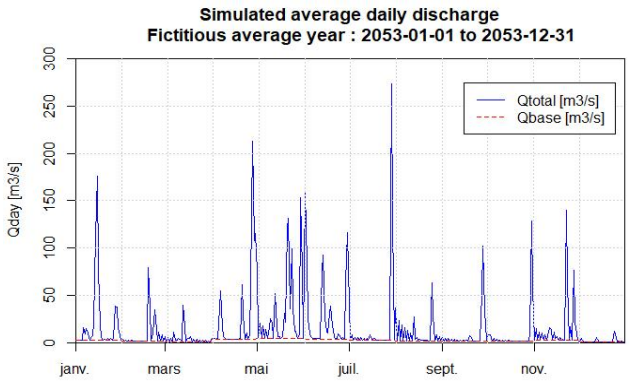

Figure 11. Average daily flows for the fictitious average year (year 2053)

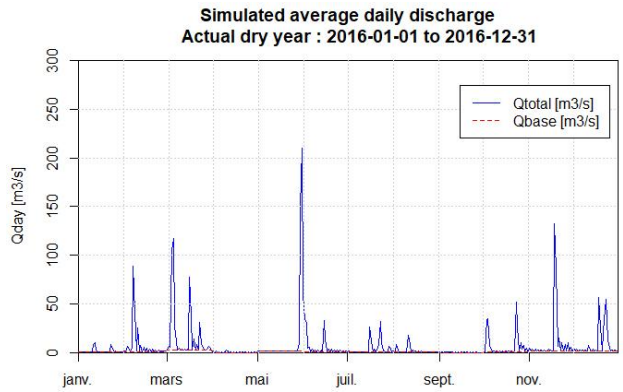

Figure 12. Average daily flows for the actual dry year (year 2016)

5. Discussions

5.1. Concerning the Data and Tools Used

The data used in this work (physical characterisations, meteorological data) are data commonly used by the scientific community and their spatial resolution is sufficiently high, 29 m for the DTM and 10 m for the LULC, to consider them as very representative of the physical reality of the watershed.

As regards the computer tools used (R, HEC-HMS), these are also fairly widely used tools, even if other tools could also have been used for this study. In addition to the fact that it is free of charge, the choice of HEC-HMS seemed to us to be largely justified by its capacity to model and reproduce the model and the sub-models used in this study, namely a conceptual model with a physical basis. It has also been successfully used and continues to be used for ungauged catchments for decades by different researchers such as [22] in India, [23] in Indiana (USA), [24] in Morocco, [25] in India, [26] in Malaysia, [27] in Central Europa etc.

5.2. Concerning the Processing of Rainfall Data

Considering mainly the three years 2000, 2016 and 2053 allows for long-term operation under either "average" or "dry" conditions, the latter being critical from a safety perspective. Indeed, in the future, even if weather conditions change from one year to the next, it is unlikely that these changes will significantly affect the conditions of an average year, especially with the way the fictitious year 2053 was constructed.

5.3. Concerning the Method of Calculating PET and AET

In the present study, the Hamon method was used ([11], [13]) mainly because of the availability of data that this method requires. The most recommended method is the so-called FAO56-PM method derived from the Penman-Monteith equation and standardised by FAO ([28], [29]). Studies by [30], on 7 years of daily data concluded that the standard error of the Hamon method compared to FAO56-PM is 0.25 mm/month, which is quite negligible.

5.4. On Hydrological Modelling

The results of the method are dependent on the regional parameter λ as it conditions the initial abstraction I_a and thus the storage capacity of the catchment (equation (5)). Although other researchers have found that it can be as λ = 0.05 [31], in the absence of field measurements to assess this, the value used in this study, λ = 0.2, was justified as we are in average conditions. Indeed, a low value of λ means a low storage capacity before the runoff, so there is a risk of having overestimated flows at the outlet, which can be misleading and therefore unsafe in relation to the objectives of this study.

Regarding routing, the parameters K and X were also evaluated at average values (K=0.5 and X=0.25) knowing that K has a value reasonably close to the travel time of a wave on the reach (Song et al., 2011) while X a measure of the degree of storage in the river and varies from 0 (maximum storage) to 0.5 (no storage but pure transmission). It must be recognised that field measurements of river morphology would have allowed the values of K and X to be set much more precisely.

5.5. On the Final Results

Interpretation of the shape of the daily flow hydrographs

Figures 10, 11 and 12 are very different from each other, but all three show a highly dissected appearance which is

characteristic of a low base flow and individualised floods. This is due to the fact that the flow is not regulated by groundwater because the basin is practically impermeable as shown in the hydrological soil class map (Figure 3).

Characteristic statistical values

The main characteristic values of the temporal flow distributions are summarised in the table below:

Table 5. Statistics on average daily flows (m3/s)

	2000	2016	2053
Minimum	0.11	0.01	0.20
1st quartile	0.82	0.51	1.60
Median	3.02	1.38	3.63
Mean	17.87	6.53	15.13
3rd quartile	11.62	2.96	9.95
Maximum	520.1	209.8	274.0

The values in this table can be interpreted as follows:

- For half of the year, i.e. for 183 days (consecutive or not), the flows are below the median (3.02 m3/s for 2000, 1.38 m3/s for 2016 and 3.63 m3/s for 2053).
- The average daily flow reaches values of 11.62 m3/s for 2000, 2.69 m3/s for 2016 and 9.95 m3/s for 2053 (values corresponding to the 3rd quartile) for only 91 days (consecutive or not) in the year.
- The mean values (17.87 m3/s for 2000, 6.53 m3/s for 2016 and 15.15 m3/s for 2053) are well above the median or even the 3rd quartile, which means that these values are only reached on a number of days during the year (probably less than 60 days). These high values of the mean were simply caused by the high values of the flood flows compared to the other (near-zero) flows seen in the figures, thus providing an important weighting.

Comparison with historical values

In view of studies for hydroelectric development, flow measurements were carried out between 1962 and 1974 at the outlet of a 196 km2 catchment area located in the north-eastern part of the Efaho basin, at the station known as Fanjahira [1]. In relation to the catchment area studied at present, this Fanjahira catchment area corresponds approximately to the whole of the SBV1, SBV2, SBV4 and SBV9 sub-catchment areas, totalling an area of 203 km2 and whose outlet is noted J2 (see Figure 9). Qualitatively, the results of this assessment are more or less the same as those reported in the present study and commented on above. Nevertheless, there are quite significant differences when comparing the quantitative results as shown in Figure 13 and Table 6 below:

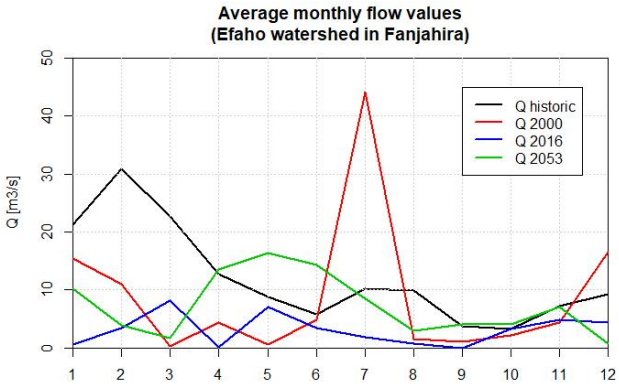

Figure 13. Comparison of monthly average flows with historical data

Table 6. Comparison of monthly average flows [m3/s]

Month	Q historical	2000	2016	2053	Month	Q historical	2000	2016	2053
J	21.3	15.4	0.6	10.3	**A**	9.86	1.5	0.7	3.0
F	30.9	11.0	3.4	3.8	**S**	3.65	1.1	0.0	4.0
M	22.7	0.2	8.1	1.7	**O**	3.25	2.1	3.2	4.0
A	12.8	4.4	0.1	13.6	**N**	7.24	4.3	4.9	7.1
M	8.73	0.6	7.0	16.4	**D**	9.25	16.5	4.3	0.7
J	5.81	4.9	3.4	14.4					
J	10.2	44.1	1.9	8.5	**Mean**	**12.14**	**8.84**	**3.15**	**7.28**

The differences between these monthly average values can be explained by several reasons, the most important of which are:

1. The historical data (1962-1974) were obtained from an annual rainfall of 3100 mm (over 196 km2) whereas the rainfall data used (1998-2019) showed a maximum value of 1540 mm (in 2005) over a BV of 503 km2 (Figure 05 and Table 3). It is therefore not surprising that the historical values are higher.
2. The methods used are significantly different: the historical values seem to have been obtained from exclusively statistical treatments, whereas in the present study the flows have been obtained from reconstructions of the physical processes taking place in the catchment area.
3. The notion of average year is also different: for historical values, the monthly averages were calculated from all monthly values of the whole period (1962-1974), whereas in the present study the average year was defined either from the interannual values of the rainfall 1998-2019 (actual average year 2000) or from a month-by-month composition of the monthly average values (fictitious average year 2053).

4. In addition, to obtain the monthly average value described in Figure 13 and Table 6 for the years 2000, 2016 and 2053, the average values were aggregated from the daily values.
5. According to Figure 5, there is a general downward trend in annual rainfall over time, which explains why in Figure 13 the average curves for 2000 and 2053 are generally below the historical average curve.

5.6. Choosing an Average Year for Hydraulic Operation

In terms of hydraulic use of the flows generated at the outlet, the fictitious average year (2053) can be a good representation of the catchment potential. In this case, the flow to be based on would be the flow corresponding to the 1st quartile, i.e. 1.60 m3/s (guaranteed for 274 days). Indeed, the actual dry year 2016 is too pessimistic while the actual average year 2000 is only the average over the period considered (1998 to 2019) but this will certainly no longer be the case in the years to come.

6. Conclusions

The present study was concerned with the assessment of the hydrological resources of the Efaho catchment. Free data were used for hypsometry, hydrography, land use, land cover, pedology and meteorological data. The assessment was based on the reconstruction of the physical processes (evapotranspiration, infiltration, runoff, routing) that give rise to the hydrograph of daily flows at the outlet.

For this assessment, the method for transforming rainfall into runoff was the SCS-CN method and the SCS unit hydrograph. For the routing method, the so-called Muskingum method was chosen. The implementation of the defined model was carried out with the HEC-HMS software and the computer programs were coded with the R language.

Throughout this study, flows for a dry year (2016) and two average years (real average year 2000 and fictitious average year 2053) were calculated. Likewise, the parameters used were average parameters, particularly with regard to the Muskingum K and X parameters.

Finally, a comparison with historical data was made for a fraction of the catchment area. This comparison showed that the same conclusions were reached from a qualitative point of view, but quite different from a quantitative point of view due to different assumptions and methods.

We recommended considering the average fictitious year 2053 for a hydraulic exploitation of the generated flows. However, in the absence of field measurements, the results of the present study are theoretical and the rainfall-discharge transformation models are uncalibrated models. An undeniable improvement of these models would be to carry out flow measurements at the outlet, which would make it possible to calibrate the real value of the parameters instead of simply considering average values.

REFERENCES

[1] P. Chaperon, J. Danloux and L. Ferry (1993). *Fleuves et Rivières de Madagascar*. Ed. ORSTOM, Paris (France), 883p.

[2] Bloschl, G. (2006). 133: Rainfall-runoff Modeling of Ungauged Catchments. *Encyclopedia of Hydrological Sciences*. Edited M G Anderson. https://doi.org/10.1002/0470848944.hsa140.

[3] Narbondo S., A. Gorgoglione, M. Crisci, C. Chreties (2020). Enhancing Physical Similarity Approach to Predict Runoff in Ungauged Watersheds in Sub-Tropical Regions. *Water* 2020, 12, 528; https://doi.org/10.3390/w12020528.

[4] Comini U.B., D.D. Da Silva, M.C. Moreira, F.F. Pruski (2020). Hydrological modelling in small ungauged catchments. *Annals of the Brazilian Academy of Sciences*, (2020) 92(2): e20180687 https://doi.org/10.1590/0001-3765202020180687.

[5] Petroselli A., R. Piscopia, S. Grimaldi (2020). Design discharge estimation in small and ungauged basins: EBA4SUB framework sensitivity analysis. *Journal of Agricultural Engineering*, 2020; volume LI: 1040, https://dx.doi.org/0.4081/jae.2020.1040.

[6] Rao K.N. (2020). Analysis of surface runoff potential in ungauged basin using basin parameters and SCS‑CN method. *Applied Water Science* (2020) 10:47.https://doi.org/10.1007/s13201-019-1129-z.

[7] Karra K., C. Kontgis, Z. Statman-Weil, J. Mazzariello., M. Mathis, S. Brumby (2021). Global land use/land cover with Sentinel-2 and deep learning. *International Geoscience and Remote Sensing Symposium* (IGARSS), IEEE, 2021.

[8] Ross C.W., L. Prihodko, S. Kumar, W. JI, N.P. Hanan (2018). Global Hydrologic Soil Groups (HYSOGs250m) for Curve Number-Based Runoff Modeling, Oak Ridge, Tennessee, USA, https://doi.org/10.3334/ORNLDAAC/1566.

[9] Goddard Earth Sciences Data and Information Services Center (2016), TRMM (TMPA-RT) Near Real-Time Precipitation L3 1 day 0.25 degree × 0.25 degree V7, Edited by Andrey Savtchenko, Greenbelt, MD, *Goddard Earth Sciences Data and Information Services Center* (GES DISC), Accessed: 2021-09-12, https://doi.org/10.5067/TRMM/TMPA/DAY-E/7.

[10] Beaudoing H., M. Rodell, NASA/GSFC/HSL (2020), GLDAS Noah Land Surface Model L4 monthly 1.0 × 1.0 degree V2.1, Greenbelt, Maryland, USA, Goddard Earth Sciences Data and Information Services Center (GES DISC), Accessed: 2021-09-12, https://doi.org/10.5067/LWTYSMP3VM5Z.

[11] Rodell M., P.R. Houser, U. Jambor, J. Gottschalck, K. Mitchell, C. Meng, K. Arsenault, B. Cosgrove, J. Radakovich, M. Bosilovich, J.K. Entin, J.P. Walker, D. Lohmann, D. Toll (2004). The Global Land Data Assimilation System, *Bulletin of American Meteorologic Society*, 85, pp. 381-394, https://doi.org/10.1175/BAMS-85-3-381.

[12] Allen R.G., L.S. Pereira, D. Raes, M. Smith (1998). "*Crop Evapotranspiration: Guidelines for Computing Crop Water*

Requirements. FAO Irrigation and Drainage Paper 56", FAO-Food and Agriculture Organization of the United Nations Rome: Rome, Italy. Avalaible on http://www.fao.org/3/x0490e/x0490e00.htm.

[13] Lang D., J. Zheng, J. Shi, F. Liao, X. Ma, W. Wang, X. Chen, M. Zhang (2017). A Comparative Study of Potential Evapotranspiration Estimation by Eight Methods with FAO Penman–Monteith Method in Southwestern China. *Water* 2017, 9, 734. https://dx.doi.org/10.3390/w9100734.

[14] Wang D., L. Qin, B. Chang, M. Wang, W. Zhang (2015). "Application of SCS-CN Model in Runoff Estimation", ISM3E: *International Symposium on Material, Energy and Environment Engineering*. https://doi.org/10.2991/ism3e-15.2015.14.

[15] Santikari V.P., L.C. Murdoch (2018). Including effects of watershed heterogeneity in the curve number method using variable initial abstraction. *Hydrology and Earth System Sciences*, 22, pp. 4725–4743, 2018. https://doi.org/10.5194/hess-22-4725-2018.

[16] USDA (1986). "*Urban Hydrology for Small Watershed, Technical Release TR-55*", 210-VI-TR-55, Second Ed. (June 1986).

[17] Ouédraogo W.A.A., J.M. Raude, J.M. Gathenya (2018). Continuous Modeling of the Mkurumudzi River Catchment in Kenya Using the HEC-HMS Conceptual Model: Calibration, Validation, Model Performance, Evaluation and Sensitivity Analysis. *Hydrology* 2018, 5, 44;https://doi.org/10.3390/hydrology5030044.

[18] USACE (2000). "*Hydrologic Modeling System HEC-HMS: Technical Reference Manual*", Hydrologic Engineering Center (2000).

[19] Samuel J., P. Coulibaly, R.A. Metcalfe (2012). Identification of rainfall–runoff model for improved baseflow estimation in ungauged basins. *Hydrological Processes*, 26, pp 356-366, https://doi.org/10.1002/hyp.8133.

[20] Laoucheria F., S. Kechida, M. Chabi (2018). "Estimation of the Parameters of Muskingum Methods for the Prediction of the Flood Depth in the Moudjar River Catchment", *International Journal of Urban and Civil Engineering*, vol. 12, No: 10. https://doi.org/10.5281/zenodo.1474811.

[21] Ehteram M., F.B. Othman, Z.M. Yaseen, H.A. Afan , M.F. Allawi, M.B.A. Malek, A.N. Ahmed, S. Shahid, V.P. Singh, A. El-Shafie (2018). "Improving the Muskingum Flood Routing Method Using a Hybrid of Particle Swarm Optimization and Bat Algorithm", *Water*, vol. 10 (807), pp.1-21, https://doi.org/10.3390/w10060807.

[22] Meenu R., S. Rehana, P.P. Mujumdar (2013). Assessment of hydrologic impacts of climate change in Tunga–Bhadra river basin, India with HEC-HMS and SDSM. *Hydrological Processes* 27, pp 1572–1589 (2013). https://doi.org/10.1002/hyp.9220.

[23] Jeon J.H., K.J. Lim, B.A. Engel (2014). Regional Calibration of SCS-CN L-THIA Model: Application for Ungauged Basins. *Water* 2014, 6, pp 1339-1359; https://doi.org/10.3390/w6051339.

[24] Ahbari A., L. Stour, A. Agoumi, N. Serhir (2018). Estimation of initial values of the HMS model parameters: application to the basin of Bin El Ouidane (Azilal, Morocco). *Journal of Materials and Environmental Sciences*, 2018, 9 (1), pp. 305-317. https://doi.org/10.26872/jmes.2018.9.1.34.

[25] Koneti S., S.L. Sunkara, P.S. Roy (2018). Hydrological Modeling with Respect to Impact of Land-Use and Land-Cover Change on the Runoff Dynamics in Godavari River Basin Using the HEC-HMS Model. *ISPRS International Journal of Geo-Information*, 2018, 7, 206; https://doi.org/10.3390/ijgi7060206.

[26] Adilah N., S. Nuramirah (2019). Estimating flow rate in gauged and ungauged stations in Kuantan river basin using Clark method in HEC-HMS. *IOP Conferences Series: Earth and Environmental Science*, 244 (2019) 012014, https://doi.org/10.1088/1755-1315/244/1/012014.

[27] Caletka M., M.S. Michalková, P. Karásek, P. Fucík (2020). Improvement of SCS-CN Initial Abstraction Coefficient in the Czech Republic: A Study of Five Catchments. *Water* 2020, 12, 1964; https://doi.org/10.3390/w12071964.

[28] Cordova M., G. Carrillo-Rojas, P. Crespo, B. Wilcox, R. Celleri (2015). Evaluation of the Penman-Monteith (FAO 56 PM) Method for Calculating Reference Evapotranspiration Using Limited Data. *Mountain Research and Development* (*MRD*), Vol 35 No 3, Aug. 2015, pp. 230–239, https://dx.doi.org/10.1659/MRD-JOURNAL-D-14-0024.1.

[29] Moratiel R., R. Bravo, A. Saa, A.M. Tarquis, J. Almorox (2020). Estimation of evapotranspiration by the Food and Agricultural Organization of the United Nations (FAO) Penman–Monteith temperature (PMT) and Hargreaves–Samani (HS) models under temporal and spatial criteria – a case study in Duero basin (Spain). *Natural Hazards and Earth System Sciences*, 20, 859–875, 2020. https://doi.org/10.5194/nhess-20-859-2020.

[30] Alkaeed O., C. Flores, K. Jinno, A. Tsutsumi (2006). "Comparison of Several Reference Evapotranspiration Methods for Itoshima Peninsula Area, Fukuoka, Japan", *Memoirs of the Faculty of Engineering*, Kyushu University, Vol. 66, No.1, 2006.

[31] Hawkins R.H., R. Jiang, D.E. Woodward, A.T. Hjelmfelt, J.E. van Mullem (2003). "*Runoff Curve Number Method: Examination of the Initial Abstraction Ratio*", Conference paper, https://doi.org/10.1061/40685(2003)308.